A model of wind transformation over water-land surfaces

V.N. Kudryavtsev*, V.K. Makin, A.M.G. Klein Tank, J.W. Verkaik
Royal Netherlands Meteorological Institute (KNMI)
De Bilt, The Netherlands

March 23, 2000

Abstract

A simple physical model of the wind transformation on abrupt changes in surface roughness and temperature across a coastal line is suggested. The model is based on a concept of the internal boundary layer (IBL) growth with the fetch. It consistently describes both small scale (order of 1km) and mesoscale (order of 10-100 km) evolution of the IBL. The planetary boundary layer (PBL) problem is solved using the similarity approach, which is applied for the IBL confined to the surface boundary layer. The description of the Ekman part of the PBL is based on the analytical solution of the momentum and heat balance equations. A 3-layer eddy-viscosity model of the PBL is introduced for the description of the mesoscale evolution of the IBL. The PBL model takes into account the baroclinicity effects due to the temperature gradient across a coastal line. The model is verified against existing data of the wind transformation across the Dutch coast of the North Sea and a reasonable agreement with observations is obtained. The model can be used as a module in multi-component coupled models describing dynamical processes in the ocean and the atmosphere and is viewed as a tool for engineering applications in the coastal zone.

1 Introduction

When wind blows from land to the sea or from sea to the land, the atmospheric boundary layer undergoes significant transformation due to abrupt changes in roughness and temperature across the water-land boundary. The Internal Boundary Layer (IBL) develops with fetch on spatial scales of about 100 km. During the initial stage, with fetches of about 1 km, the IBL growth is confined to the Surface Boundary Layer (SBL). During later stages the IBL penetrates the top of the SBL and develops further in the Ekman part of the Planetary Boundary Layer (PBL).

*On leave from the Marine Hydrophysical Institute, Sevastopol, Crimea, Ukraine

A proper description of wind fields in the coastal zone is important for many applications in ocean and atmosphere modelling. It is a known property of storm surge models to underpredict surges in off-shore wind conditions. Inadequate description of coastal winds can cause this underprediction. Modelling of wind wave evolution near the coast requires knowledge of coastal wind fields. Inadequate interpolation of winds in the coastal zone can cause significant errors in the description of wave evolution and propagation in wave prediction models. The calculation of the exchange coefficient of momentum, heat, water vapor and gases in the coastal zone also requires accurate estimates of coastal winds. Correct estimates of wind fields over land characterized by varying roughness and/or over small inland waters (lakes, estuaries) are very important to numerous engineering applications.

The description of the wind transformation requires a solution of the planetary atmospheric boundary layer problem. The PBL is formed by a combined effect of the Coriolis force and the turbulent stress. The latter is a result of the dynamical and thermal interaction of the air flow with the underlying surface.

Major efforts to study the evolution of the PBL were made by numerical modelling studies based on the solution of the Reynolds equations. Reynolds stresses have been parametrized by various closure hypotheses such as two-equation eddy-viscosity schemes and second order turbulent-stress models (Venkatram, 1977; Garratt, 1987; Garratt et al., 1996). The application of large-eddy simulations of the PBL is rapidly evolving (Deardorff, 1972; Mason, 1994; Garratt et al., 1996). However, these models are very expensive and their use is limited to specific scientific problems. Simpler models of the PBL which are based on the ideas of similarity theory by Kazansky and Monin (1960) and some empirical knowledge (Brown, 1982; Garratt, 1987; Van Wijk et al., 1990; Zilitinkevich, 1989 a,b; Kudryavtsev, 1995; Kudryavtsev and Makin, 1996) are more attractive for engineering applications.

The main goal of the present paper is to revise and extend the simplified model of the wind transformation in the coastal zone developed by Kudryavtsev and Makin (1996) (hereafter KM96-model). It is based on the two-layer PBL model suggested by Brown (1982), which is generalised by accounting for the vertical distribution of the eddy-viscosity coefficient in the PBL in the presence of the IBL. The model is a semi-empirical one and is based on similarity theory of the surface boundary layer and the analytical description of the Ekman layer. It is viewed as a tool for engineering applications.

The extended model is capable of describing the PBL evolution in the multi-transition case, that is, when the air flow crosses several surfaces characterized by different roughness and temperature. It is applied for the description of the wind transformation across the Dutch coast of the North Sea, over the land, and over the inland lake Markermeer. Results are compared with the wind speed measurements performed at several meteo-stations in North Holland (De Kooy, Wijdenes, Houtrib, and Lelystad). These stations are situated roughly on a line which coincides with a wind direction of about 310^o (northwestern winds) and crosses the coast of the North Sea, the land, and the inland water basin (Markermeer lake). The comparison between model results and data is found to be reasonably good as far as the average wind speed is concerned. Accounting for stratification effects in the model does not seem to improve the correlation between the measured and modelled wind speed at inland stations. Though, the scatter in the data does not seem to be caused by stratification

effects either. The scatter is most probably caused by synoptic variability of the atmosphere.

The model is presented in section 2. The two-layer model of the PBL by Brown (1982), and the extensions made to this model by the authors, are described in sections 2.1 and 2.2. Then a set of equations is derived by which wind and temperature profiles in the IBL can be calculated. The transformation of the PBL under single and multiple land-sea or sea-land transitions, respectively is described in sections 2.4 and 2.5. Section 3 describes the comparison of model results with observations, and some conclusions are made in section 4.

2 Model of the PBL Transformation

The transformation of the atmospheric planetary boundary layer, forced by the step change in the surface roughness, temperature or humidity, is described using an internal boundary layer approach. The IBL is associated with horizontal advection of air across the discontinuity in some property of the surface. It is defined as the lower part of the PBL where the structure of turbulence is modified due to interactions with the surface.

Two main regimes are distinguished in the growth of the IBL. The small scale evolution of the IBL takes place on small fetches (few kilometres from the coast), where the growth of the IBL is confined to the surface boundary layer. Mesoscale evolution takes place on scales from few kilometres to few hundreds kilometres depending on the atmospheric stratification. During this stage the IBL penetrates the top of the SBL and evolves in the Ekman part of the PBL. A comprehensive review of the IBL problem is given, for example, by Garratt (1990). The present model is based on the 3-layer PBL model by Kudryavtsev and Makin (1996).

2.1 Background Model

Brown (1982) proposed a very simple two-layer model of the equilibrium (background) PBL which consists of the lower surface boundary layer of height h and the upper Ekman boundary layer (EBL) of height D. The SBL is described in terms of the Monin-Obukhov similarity theory. The eddy-viscosity coefficient K increases with height within this layer according to:

$$K = \frac{\kappa u_* z}{\Phi_u(z/L)}. \tag{1}$$

The eddy-viscosity coefficient in the Ekman part of the PBL ($z > h$) is assumed to be constant with height and is equal to its value at the upper boundary of the SBL $z = h$:

$$K_h = \frac{\kappa u_* h}{\Phi_u(h/L)}, \tag{2}$$

where $\kappa = 0.4$ is the von Karman constant, u_* is the friction velocity, $L = -u_*^3/(\kappa\beta q_s)$ is the Monin-Obukhov length scale, q_s is the surface kinematic heat flux, β is the buoyancy parameter, Φ_u is the universal similarity function (the dimensionless gradient of the wind profile, see Appendix 6.1).

The eddy-viscosity K defines the vertical scale of the PBL or the Ekman depth

$$H = \left(\frac{2K_h}{f}\right)^{1/2} = \frac{\kappa u_*}{f}\Lambda(\mu), \tag{3}$$

where $\mu = \kappa u_*/fL$ is the stratification parameter. $\Lambda(\mu)$ is a dimensionless function which satisfies the equation

$$\Lambda(\mu) = \frac{2\varepsilon}{\Phi[\varepsilon\mu\Lambda(\mu)]} \tag{4}$$

where $\varepsilon \sim 0.1$ is the main fitting parameter of the model by Brown (1982) (in our model we take $\varepsilon = 0.15$). This parameter defines the SBL height via the PBL scale H

$$h = \varepsilon H. \tag{5}$$

The height of the PBL is also defined via the Ekman depth H: $D = mH$, where constant m equals 2.

According to the Monin-Obukhov similarity theory wind and temperature profiles in the SBL ($z < h$) are

$$\mathbf{U}(z) = \frac{\mathbf{u}_*}{\kappa}\left[\ln(\frac{z}{z_0}) - \Psi_u(z/L)\right], \tag{6}$$

$$\theta(z) = \theta_s + \frac{\theta_*}{\kappa}\left[\ln(\frac{z}{z_0 t}) - \Psi_\theta(z/L)\right], \tag{7}$$

where $\mathbf{u}_* = u_* \exp(i\varphi_s)$, φ_s is the surface wind direction relative to the perpendicular to the coastal line, θ_s is the surface temperature, $\theta_* = -q_s/u_*$ is the scale of temperature, z_0 and z_{0t} are roughness scales for velocity and temperature respectively, and Ψ_u and Ψ_θ are universal empirical functions specified in Appendix 6.1. Wind and temperature profiles in the Ekman part of the PBL ($h < z < D$) result from the solution of the primitive conservation equations of momentum and heat under stationary and spatially homogeneous conditions:

$$\mathbf{U}(z) - \mathbf{G} = -(1-i)\Lambda^{-1}(\mu)\frac{\mathbf{u}_*}{\kappa}\frac{\sinh\left((1+i)(m - z/H)\right)}{\cosh((1+i)(m-\varepsilon))}, \tag{8}$$

$$\theta(z) - \theta_D = -\frac{\theta_*}{\kappa}\Lambda^{-1}(\mu)(m - z/H), \tag{9}$$

where $\mathbf{G} = G\exp(i\varphi_g)$ is the geostrophic wind, φ_g is its direction, θ_D is the potential temperature at the upper boundary of the PBL. Wind and temperature profiles in the SBL ((6), (7)) and in the PBL ((8), (9)) should be continuous at $z = h$. This condition defines the resistance laws of the PBL

$$\frac{\kappa(\theta_D - \theta_s)}{\theta_*} = \ln\left(\frac{\kappa u_*}{f z_{0t}}\right) - C(\mu), \tag{10}$$

$$\frac{\kappa\mathbf{G}}{\mathbf{u}_*} = \ln\left(\frac{\kappa u_*}{f z_0}\right) - B(\mu) - iA(\mu). \tag{11}$$

Here $A(\mu)$, $B(\mu)$ and $C(\mu)$ are the universal functions defined as

$$A(\mu) = \Lambda^{-1}(\mu)\tanh((1+i)(m-\varepsilon)), \quad (12)$$

$$B(\mu) = -A(\mu) + \Psi_u(\varepsilon\mu\Lambda(\mu)) - \ln(\varepsilon\Lambda(\mu)), \quad (13)$$

$$C(\mu) = -2\Lambda^{-1}(\mu)(m-\varepsilon) + \Psi_\theta(\varepsilon\mu\Lambda(\mu)) - \ln(\varepsilon\Lambda(\mu)). \quad (14)$$

The resistance laws relate parameters of the free atmosphere at the upper boundary of the PBL to the surface heat flux and the surface stress vector.

2.2 Internal Boundary Layer Depth

According to the definition the internal boundary layer is the lower part of the planetary boundary layer where the disturbances of turbulent characteristics caused by abrupt changes in underlying surface parameters (roughness, temperature, and humidity) are confined. The IBL depth δ grows with time or with fetch.

The extension of the two-layer model of Brown (1982) is mainly related to the additional assumptions concerning the vertical distribution of the eddy-viscosity coefficient K. The IBL can develop both in the SBL and the EBL, and its parameters differ from the parameters of the background atmosphere. So, we define the eddy-viscosity as

$$K = \begin{cases} K(z,\mu,u_*) & \text{if } z < \delta \\ K_0(z,\mu_0,u_{*0}) & \text{if } z > \delta(x) \end{cases}, \quad (15)$$

where the subscript 0 denotes parameters of the background PBL, K and K_0 on the right hand side of this equation are defined by equation (1) or (2) depending on the relation between δ and the SBL height h or h_0 (in the case of the thermal IBL, the turbulent heat transfer has the same form as (1) or (2) where $\Phi_u(z/L)$ is replaced by $\Phi_\theta(z/L)$). Hence, the eddy-viscosity coefficient in the IBL is defined by the local heat and momentum fluxes.

In many problems concerning the evolution of turbulent boundary layers, the growth rate of a turbulent region (or small disturbances inside turbulent flows) can be estimated as

$$U_\delta \frac{\partial \delta^2}{\partial x} \sim K(\delta) \quad (16)$$

where $U_\delta = U(\delta)$, and $K(\delta)$ is the eddy-viscosity at $z = \delta$. For example, the scale of the inner region l (or the IBL in our terminology) of the turbulent air flow over periodic surface waves (or hills) with the wavenumber k is

$$l \sim \frac{\kappa u_*}{k U_l} \quad (17)$$

(see Belcher and Hunt, 1993). Relation (17) results from (16) if $K(\delta) = \kappa u_* \delta$ and $\partial/\partial x$ is replaced by k. The height of the turbulent boundary layer developing over the flat surface at high Reynolds number also follows from equation (16) at $K(\delta) = \kappa u_* \delta$:

$$\frac{\partial \delta}{\partial x} \sim \kappa \frac{u_*}{U_\delta}, \quad (18)$$

$$\delta = \frac{\kappa^2}{\ln(\delta/z_0)} X \quad (19)$$

where X is the fetch. Relation (19) agrees well with laboratory experiments (e.g., Bradley, 1968; Garratt, 1990). Equation (16) is valid also for the description of the stratified turbulent flow evolution inside the neutral flow. However, in this case the eddy-viscosity coefficient should be replaced by the heat conductivity coefficient, which depends on the stratification parameter. Such approach was used by Jensen et al (1984) and by Van Wijk et al. (1990) for the description of the IBL height at small fetches of a few kilometres.

From the physical point of view the same equation (16) can be used to estimate the rate of the IBL growth when its height exceeds the SBL thickness and the IBL develops inside the Ekman part of the PBL. What has to be taken into account is that the eddy-viscosity coefficient is independent of height (but its value depends on the stratification parameter). Further we shall use equation (16) to define the height of the IBL developing inside the neutrally stratified background atmosphere under an abrupt change of the surface temperature and surface roughness. We rewrite equation (18) in the form

$$U_\delta \frac{\partial \delta^2}{\partial x} = 4K(\delta) \tag{20}$$

with $K(\delta)$ defined by (1) if $\delta < h$, and by (2) if $\delta > h$ where h is the local SBL height. In equation (16) the proportionality coefficient 4 is chosen to fit the model to empirical data (see, KM96).

The only exceptional case which cannot be described by equation (20) is the development of the convective IBL inside a stably stratified atmosphere. It is known (e.g., Tennekes, 1973; Venkatram, 1977; Garratt, 1990) that when the convective IBL develops in a weakly turbulent stably stratified atmosphere, the inversion temperature jump is formed at its upper boundary. The temperature jump is usually parameterized as

$$\Delta\theta \equiv \theta_0(\delta) - \theta(\delta) = \epsilon\gamma_0\delta, \tag{21}$$

where ϵ is a constant and γ_0 is the lapse rate in the background (undisturbed) atmosphere. The heat flux from the background atmosphere to the IBL due to the entrainment of warmer air into the IBL is

$$q_\delta = -\Delta\theta U_\delta \frac{\partial \delta}{\partial x}. \tag{22}$$

In a well mixed convective IBL the vertical change in temperature is negligible. Then the IBL heat balance equation has the form (e.g., KM96)

$$U_\delta \left(\gamma_0 \delta \frac{\partial \delta}{\partial x} - \delta \frac{\partial}{\partial x} \Delta\theta \right) = q_s - q_\delta. \tag{23}$$

With (21) and (22), equation (23) reduces to

$$U_\delta \frac{\partial}{\partial x} \delta^2 = \frac{2}{1 - 2\epsilon} \frac{q_s}{\gamma_0}, \tag{24}$$

which describes the growth of the convective IBL. From equation (24) the entrainment heat flux can be derived as:

$$q_\delta = -\frac{\epsilon}{1-2\epsilon} q_s. \tag{25}$$

Equation (25) corresponds to the one of the convective IBL model by Tennekes (1973). The constant ϵ varies in the range of $0.15 \div 0.25$ according to experimental data and results of the numerical modelling . If we take $\epsilon = 0.25$, then equation (24) is

$$U_\delta \frac{\partial}{\partial x}\delta^2 = 4\frac{q_s}{\gamma_0}. \tag{26}$$

Equations (20) and (26) describe different regimes of the IBL growth. In real conditions the IBL develops both due to abrupt changes in roughness and surface temperature. The stratification of the background atmosphere can be arbitrary and influences the IBL growth. To describe the wind transformation in real conditions it is desirable to have a uniform description of the IBL growth. We introduce the following generalized equation for the growth of the IBL height

$$U_\delta \frac{\partial}{\partial x}\delta^2 = 4\alpha K(\delta), \tag{27}$$

with $K(\delta)$ defined by (1) if $\delta < h$, and by (2) if $\delta > h$. Here α is the growth rate parameter which has to provide a smooth transition of the IBL growth from one regime to another. We specify the growth rate parameter as (for details see Kudryavtsev and Makin (1996))

$$\alpha = \frac{1 + \max(\gamma_0 K_0/q_s, 0)}{1 + \max(\gamma_0 K/q_s, 0)} \tag{28}$$

where K_0 is the eddy-viscosity coefficient in the background atmosphere. It has the following asymptotic regimes: a) when $\gamma_0 \simeq 0$ (the background atmosphere is unstable or near-neutral), then $\alpha = 1$, and equation (27) takes the form (20); b) if the stably stratified IBL develops inside the stable atmosphere, then $\alpha = 1$. This again corresponds to the regime described by (20); c) if the convective IBL develops in the stably stratified atmosphere then $\alpha_\gamma \simeq q_s/(\gamma_0 K)$ which correspond to the regime described by (26).

The eddy-viscosity coefficient has different height dependence in the SBL and in the EBL, equations (1) and (2). From (27) it follows that at small fetches when the IBL develops inside the SBL (small scale IBL evolution) its height grows as $\delta \sim x$, while at large fetches when the IBL evolves in the EBL (mesoscale IBL evolution) its height grows as $\delta \sim x^{1/2}$. The transition from the small scale evolution to the mesoscale evolution occurs when the dimensionless fetch

$$xf/G \simeq \varepsilon^2,$$

which normally does not exceed a few kilometres.

Below we illustrate how the IBL height, which follows from equation (27) is related to results from experimental studies of the mesoscale evolution of the IBL, i.e., when the wind fetch is of order 10 km or more.

Convective IBL. A comprehensive review of experimental studies of the convective IBL growth can be found, for example, in Garratt (1990). The wind-tunnel study by Meroney et al. (1975) shows the square root dependence of IBL height on fetch. Raynor et al. (1975, 1979) used dimensional analysis and obtained an empirical relation which approximates closely the observed IBL heights

$$\delta = C_D^{1/2}\gamma_0^{-1/2}(\theta_l - \theta_s)^{1/2}X^{1/2}, \tag{29}$$

where $\theta_l - \theta_s$ is the temperature difference between land and sea. The empirical relation (29) is valid for the fetch from several km to about 50 km. The approximate solution of (27) for the small fetch is

$$\delta = 2C_H^{1/2}\gamma_0^{-1/2}(\theta_l - \theta_s)^{1/2}X^{1/2}, \tag{30}$$

where we used $q_s = C_H G(\theta_l - \theta_s)$. Equation (30) has the same form as (29). The difference in the proportionality coefficient results from the fact that we use the heat transfer coefficient instead of the drag coefficient to obtain the relation. Note that our relation agrees with the one by Venkatram (1977) obtained from the analysis of numerical calculations.

Stable thermal IBL. Field observations of the stably stratified IBL growth has received increased attention in recent years. The growth of the stable thermal IBL was studied by e.g. Mulhearn (1981), Garratt (1987), and Garratt and Ryan (1989). It was found that the IBL growth for fetches up to hundreds of km is relatively small (the IBL depth does not exceed a height of about 100m), and the IBL height obeys a square root dependence on X. Mulhearn (1981) has analyzed measurements of temperature and the wind speed made in the offshore flow over the Massachusetts Bay. Using dimensional analysis he suggested a relation which approximates well the available observations

$$\delta = 0.015u(g\Delta\theta/\theta)^{-1/2}X^{1/2}, \tag{31}$$

where $\Delta\theta$ is the temperature difference between the sea surface and the upstream flow. The same relation is obtained by Garratt (1987) who parameterized the results of numerical calculations.

In order to compare the model predictions of IBL depth, equation (27), with the empirical relation (31), we shall take into account the main features of the stably stratified IBL. Assuming that the IBL stratification is rather strong, we prescribe that the IBL eddy-viscosity coefficient approximately equals

$$K = \frac{1}{5}\kappa u_* L. \tag{32}$$

Taking into account this relation, the solution of equation (27) can be written as

$$\delta = C\left(\frac{g}{\overline{T}}\Delta\theta\right)^{-1/2} GX^{1/2}, \tag{33}$$

where the constant $C = [4C_D^2/(5C_H)]^{1/2}$. The model relation has the same form as the empirical one. For the stable IBL the transfer coefficients C_D and C_H are of the order of

10^{-4}, which gives $C \sim 0.02$. That is in good agreement with the empirical value 0.015 of equation (31). The model results are consistent with field observations of the stably stratified IBL height.

We conclude that equation (27) reproduces reasonably well the empirically derived relations for the IBL growth in the most important asymptotic regimes.

2.3 Wind and Temperature Profiles in IBL and Resistance Laws

In the general case, the wind velocity and potential temperature profiles in the developing IBL result from the solution of the following differential equations

$$U\frac{\partial\theta}{\partial x} = \frac{\partial}{\partial z}K_\theta\frac{\partial\theta}{\partial z}, \tag{34}$$

$$U\frac{\partial\mathbf{U}}{\partial x} + if(\mathbf{U}-\mathbf{G}) = \frac{\partial}{\partial z}K\frac{\partial\mathbf{U}}{\partial z}, \tag{35}$$

where the x-axis is directed perpendicularly to the line of an abrupt change in surface parameters, $\mathbf{U} = U + iV$ is the complex wind velocity (vector $\mathbf{U}$ coincides with the x-axis), K_θ and K are the turbulent transfer coefficients defining by equation (1) if $z < h$ or by equation (2) if $z > h$. The boundary conditions are

$$\theta(z_{0t}) = \theta_s, \tag{36}$$

$$\theta(\delta) = \theta_\delta, \tag{37}$$

$$\mathbf{U}(z_{0t}) = 0, \tag{38}$$

$$\mathbf{U}(\delta) = \mathbf{U}_\delta. \tag{39}$$

Here θ_δ and $\mathbf{U}_\delta$ are the potential temperature and the wind velocity at the upper boundary of the IBL. In zero order of accuracy, equations (34) and (35) can be reduced to the one-dimensional diffusive equations (an example of the solution of the full equations is given in KM96). The solution of these equations does not depend on fetch explicitly. The implicit dependency on fetch is realized via the spatially non-uniform surface momentum and heat fluxes.

In the case where the IBL height is less than the local thickness of the SBL (at $z < h$), the solution of one-dimensional equations (34) and (35) with the lower boundary conditions (36) and (38) are

$$\mathbf{U}(z) = \frac{\mathbf{u}_*}{\kappa}\left[\ln(\frac{z}{z_0}) - \Psi_u(z/L)\right], \tag{40}$$

$$\theta(z) = \theta_s + \frac{\theta_*}{\kappa}\left[\ln(\frac{z}{z_0 t}) - \Psi_\theta(z/L)\right]. \tag{41}$$

The diabatic profiles of the wind speed and temperature are well established over the sea and land.

In the case of mesoscale IBL evolution, the IBL develops inside the Ekman part of the PBL, where K and K_θ are constant over height. The solution of (34) and (35), which satisfies

the continuity of momentum and heat fluxes through the upper boundary of the SBL and the upper boundary conditions (37) and (39), is

$$\begin{aligned}\mathbf{U}(\zeta)-\mathbf{G} &= -(1-i)\Lambda^{-1}(\mu)\frac{\mathbf{u}_*}{\kappa}\frac{\sinh\left((1+i)d(1-\zeta)\right)}{\cosh((1+i)d)}+\\ &\quad +(\mathbf{U}_\delta-\mathbf{G})\frac{\cosh((1+i)d\zeta)}{\cosh((1+i)d)}, \qquad (42)\\ \theta(\zeta)-\theta_\delta &= -2\frac{\theta_*}{\kappa}\Lambda^{-1}(\mu)d(1-\zeta), \qquad (43)\end{aligned}$$

where $d=(\delta-h)/H$ is the dimensional parameter of the IBL height, $\zeta=(z-h)/(\delta-h)$ is the dimensionless vertical coordinate, and $\mathbf{U}_\delta$ and θ_δ are the wind velocity and temperature at the upper boundary of the IBL. Equations (41) and (43) should account for the possible temperature jump across the inversion at the top of the convective IBL

$$\theta(\delta)=\theta_0(\delta)-\epsilon\gamma_0\delta, \qquad (44)$$

where $\epsilon=\max(0,\frac{1}{4}\mathrm{sign}(q_s))$. The convective IBL develops and can become neutral or even stable. To allow for smooth transition through the point where $q_s=0$, we define ϵ_θ in the form

$$\epsilon_\theta=\max\left(0,\frac{1}{4}\frac{q_s}{\gamma_0 K}\frac{1}{\alpha}\right) \qquad (45)$$

with the IBL growth rate parameter defined by (28).

Notice again that the wind and temperature profiles in the IBL, defined by equations (40) and (41) at $z<h$ and by equations (42) and (43) at $h<z<\delta$, depend on the local heat and momentum surface fluxes. In the course of the IBL evolution the local fluxes are changing. These surface fluxes are defined by the IBL resistance laws. At small fetches (when the IBL develops in the SBL) the resistance laws follow from the condition that the wind speed and temperature profiles in the IBL have to match the wind velocity and temperature at its upper boundary. The latter are equal to their values in the background (undisturbed) PBL (in the convective IBL the temperature jump (44) has to be accounted for). So, at $\delta<h$ the resistance laws are

$$\begin{aligned}\frac{\kappa\mathbf{U}_\delta}{\mathbf{u}_*} &= \left[\ln(\frac{\delta}{z_0})-\Psi_u(\delta/L)\right], \qquad (46)\\ \frac{\kappa(\theta_\delta-\theta_s)}{\theta_*} &= \left[\ln(\frac{\delta}{z_0 t})-\Psi_\theta(\delta/L)\right]. \qquad (47)\end{aligned}$$

During the stage of mesoscale evolution, the resistance laws of the IBL result from the continuity of the wind velocity and temperature profiles at level $z=h$. Patching the wind and temperature profiles in the SBL (equations (40) and (41)) with the ones in the Ekman part of the IBL (equations (42) and (43)) we obtain the following resistance laws of the IBL

when its height exceeds h ($\delta > h$)

$$\frac{\kappa(\theta_\delta - \theta_s)}{\theta_*} = \ln\left(\frac{\kappa u_*}{f z_{0t}}\right) - C(\mu, d), \tag{48}$$

$$\frac{\kappa \mathbf{G}}{\mathbf{u}_*} = \left[\ln\left(\frac{\kappa u_*}{f z_0}\right) - B(\mu, d) - iA(\mu, d)\right]\left(1 + \frac{\mathbf{U}_\delta/\mathbf{G} - 1}{\cosh((1+i)d)}\right)^{-1}. \tag{49}$$

Here $A(\mu, d)$, $B(\mu, d)$ and $C(\mu, d)$ are universal functions defined as

$$A(\mu, d) = \Lambda^{-1}(\mu)\tanh((1+i)d), \tag{50}$$

$$B(\mu, d) = -A(\mu, d) + \Psi_u(\varepsilon\mu\Lambda(\mu)) - \ln(\varepsilon\Lambda(\mu)), \tag{51}$$

$$C(\mu, d) = -2\Lambda^{-1}(\mu)d + \Psi_\theta(\varepsilon\mu\Lambda(\mu)) - \ln(\varepsilon\Lambda(\mu)). \tag{52}$$

The resistance laws relate parameters of the undisturbed PBL at height of the IBL to the surface heat and momentum fluxes which, in turn, define the wind and temperature profiles inside the IBL.

2.4 Procedure of Model Calculations

Equations for the wind velocity and temperature profiles together with the IBL resistance laws obtained in Section 2.3 describe the PBL transformation caused by an abrupt change in surface temperature or/and surface roughness. The local IBL structure is calculated for several dimensionless IBL heights along the fetch. Then the solution for every height is related to the spatial coordinates using the equation of the IBL growth rate (27).

2.4.1 External parameters of the model

The external parameters of the model which have to be provided are:

1. The geostrophic wind speed and its direction.
2. Air temperature at any relatively high level (order of 1000 m) θ_a.
3. Temperature of land surface θ_l and sea surface θ_s.
4. Land roughness z_0.

In applications, it could be that the wind velocity and air temperature, used in the model as external parameters, are provided at any arbitrary level or even at different levels. The parameters of the background atmosphere can be then obtained by the procedure described in Appendix 6.2 and 6.3.

2.4.2 Structure of the background PBL

To initialize the model, the structure of the upwind background (undisturbed) PBL needs to be determined. It is defined by the external parameters and is calculated according to:

1. The background friction velocity u_{*0}, the surface wind speed direction ϕ_{s0}, and the temperature scale θ_{*0} are determined from the resistance laws (10) and (11).

2. The wind and temperature profiles in the SBL are obtained from equations (6) and (7), and in the Ekman part of the PBL - from equations (8) and (9). The description of the background atmosphere is hereby completed.

2.4.3 IBL structure

The IBL develops in the background atmosphere. The required input parameters are:

1. Dimensionless IBL heights $\tilde{\delta} = \delta/H$, $(d = \tilde{\delta} - \varepsilon)$ distributed along the fetch.

2. Parameters of the background atmosphere.

The IBL structure is calculated as follows:

1. The local value of the friction velocity, surface wind direction and temperature scale are obtained from the resistance laws (47) and (46) if $\tilde{\delta} < \varepsilon$ (small scale evolution), or from equations (48) and (49) if $\varepsilon < \tilde{\delta} < m$ (mesoscale evolution).

2. The local SBL height is calculated from equation (5). The local IBL depth is defined by $\tilde{\delta}$ and the PBL scale H, equation (3), as $\delta = \tilde{\delta}H$.

3. The wind and temperature profiles in the SBL follow from (40) and (41), and in the Ekman part of the IBL from (42) and (43). The growth rate parameter α is defined by (28). In the case of a convective IBL, the temperature inversion at the top of the IBL has to be taken into account by relation (44).

After the local structure of the IBL is obtained for each value of the IBL depth $\tilde{\delta}$, we need to map the solution on spatial coordinates.

2.4.4 IBL depth as a function of fetch

To map the IBL solution on the x-coordinate we have to find the relation $x = x(\tilde{\delta})$. That can be done using equation (27) describing the IBL growth rate. This equation determines x as a function of known parameters of the IBL

$$\tilde{x} = \int_{\max(z_0, z_{0b})}^{D} p^{-1} \frac{U_\delta}{G} \frac{\tilde{\delta}}{\alpha(d)} \frac{\Lambda(\mu)}{\Lambda(p\mu)} \frac{1}{H} d\delta, \tag{53}$$

where $p = \min(\tilde{\delta}/\varepsilon, 1)$ and the universal function $\Lambda(\mu)$ is defined by equation (4). Here $\tilde{x} = xf/|G|$ is the dimensionless x-coordinate which is perpendicular to the coastal line. The dimensionless fetch (along the surface wind) is calculated from $\tilde{X} = \tilde{x}/\cos\phi_s$.

After the local IBL solutions are related to the spatial coordinates the complete description of the PBL transformation in the coastal zone is achieved.

2.5 Multi-Transitions

The model presented above describes the PBL transformation across a single line of an abrupt change in surface parameters. In this case the air flow crosses two surfaces with different surface parameters. An example of such a 'single' transition can be the transformation of the PBL above water-land, land-water, cold-warm waters, or forest-farmlands surfaces. In reality the air flow can cross several surfaces characterized by different surface parameters. An example of such a 'multi' transition can be the transformation of the PBL above an island (water-island-water) or a small water basin (land-water-land). In the water-island-water case the IBL above the island develops inside the background PBL adjusted to the upwind sea surface. It grows in depth only up to the downwind side of the island. After that, the air flow runs again into the water and a 'new' IBL begins to develop inside the 'old' IBL. As the source of turbulent disturbances responsible for the old IBL growth is 'switched off' (the island has been passed), the old IBL will slowly disappear. Initially, a new actively growing IBL will develop inside the old IBL; after that it can penetrate into the background PBL. This happens if the height of the new IBL exceeds the height of the old IBL developed over the island. An example of the multi-transitional PBL evolution under real conditions (ocean frontal zone) and its analysis is given by Kudryavtsev et al., (1996).

The present model can be easily extended to describe the multi-transitional PBL evolution. We define the surfaces of different lengths L_i along the wind direction characterized by different roughnesses z_{0_i} and temperatures θ_{s_i}. The main assumption is that above each surface L_i the wind and temperature profiles are still described by equations (40) - (43), and the resistance laws by equations (46) -(49). However, in this case parameters of the background atmosphere at the IBL height $z = \delta_i$ (which are used in the resistance laws and the wind and temperature profiles) are related to the parameters of the IBL developed on the previous upwind surface (if $\delta_i < \delta_{i-1}(L_{i-1})$), or on the surface before (if $\delta_i > \delta_{i-1}(L_{i-1})$). In the case of sea-island-sea transition, the first condition corresponds to the parameters above the island, while the second condition corresponds to the parameters of the first sea surface.

Hence, the model of the multi-transitional PBL transformation can be built as a chain of IBLs following each other. Notice, that if the spatial scale L_i of a surface is comparable with G/f (this parameter characterizes the spatial scale of the IBL adjustment to a new surface), then a chain-model is not needed. In this case the IBL develops fully inside the background PBL adjusted to the upwind (previous) surface.

3 Spatial Variations of Surface Wind: Comparison With Observations

3.1 Data

Observations of wind speed and wind direction were collected for the period August 11, 1994 to January 13, 1995 from five stations situated in North Holland: IJmuiden, De Kooy, Wijdenes, Houtrib and Lelystad. The locations of these stations are shown in Figure 1. Apart from IJmuiden, the stations are located along a line which coincides with the on-shore wind direction of about 310^o (north-western winds). The analysed set contains 140 data points selected such that the wind direction falls into the interval from 295 to 325 degrees. The measurements at station IJmuiden are used to reconstruct the air flow parameters above the sea and parameters of the sea surface. We thus assume that the sea and the atmosphere on scales of a few hundred kilometres are homogeneous, and that measurements at IJmuiden are representative for background conditions for the De Kooy station. In particular, the wind speed at IJmuiden at 18 m height and the sea temperature measured at Lichteiland Goeree are used as external parameters to reconstruct the background atmosphere above the sea. Additionally, the air temperature at 850 mbar (about 1100 m) measured by the radiosonde of De Bilt is used as a reference temperature of the background atmosphere. Again, the upper atmosphere on scales of the Netherlands is assumed to be homogeneous. Other measured parameters needed to run the model are temperatures of the land surface and the Markermeer, and the land roughness. To obtain the land temperatures for North Holland measurements at Hoorn are used, for Flevoland and the Markermeer measurements at Lelystad are used. The land roughness is assumed to be 0.03 m and the Charnock relation is used for the lake roughness.

Notice that the case considered relates to the complex multi-transitional PBL evolution. The air formed over the North Sea flows over land, then over lake Markermeer and then again over land (Flevoland polder).

3.2 Analysis of Wind Observations

The time series of measured wind speed at stations De Kooy, Wijdenes, Houtrib, Lelystad are shown in Figures 2-5. To compare the evolution of wind over the land with the one over sea, the series of wind speed for the same cases at the coastal station are also plotted. The stratification parameter μ is shown in the lower plots and illustrates the atmospheric stability condition. The stratification parameter of the atmospheric boundary layer over the sea and the stratification parameter of the sea-land transition, defined as

$$\mu_{sl} = -\frac{\kappa^2 \beta(\theta_{sea} - \theta_{land})}{fU} \tag{54}$$

are also shown. Negative values of μ_{sl} correspond to warm air flow reaching the cold land. In this case a stable IBL is developed. As it follows from Figures 2-5, in most cases μ_{sl} is negative, so over North Holland in the autumn-winter period (for winds blowing from the

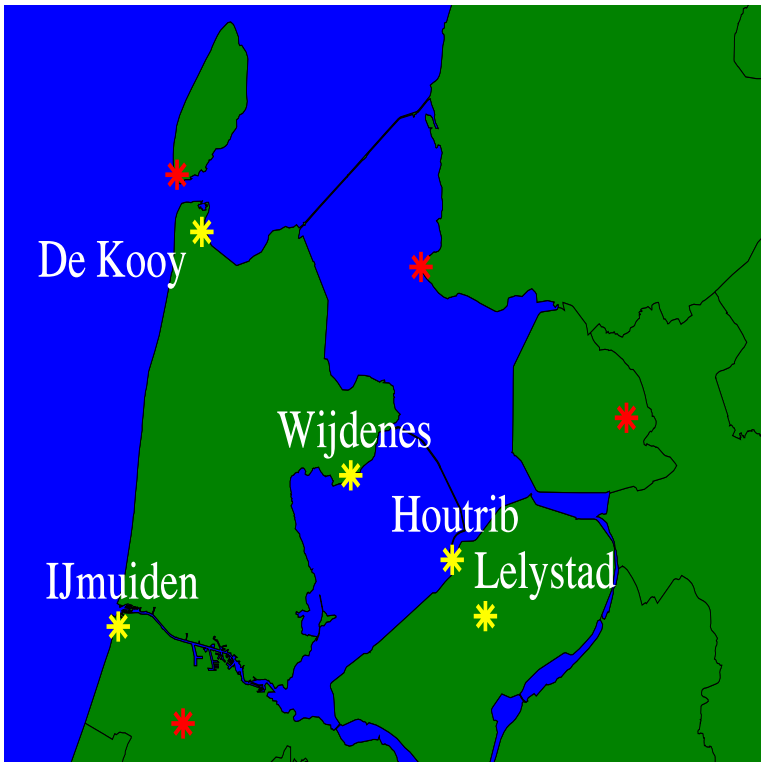

Figure 1: Location of meteo-stations

sea) the typical situation is an adjustment of warm air formed over the sea flowing over relatively cold land.

The observed wind speed at all stations follows closely the wind speed observed over the sea. However, there is a systematic difference between the wind speed over land and sea. This difference is well pronounced at stations Wijdenes and Lelystad which are characterized by long fetches. It illustrates the effect of the wind transformation. Wind accelerates over the smooth sea surface, and decelerates over the rough land; the longer the fetch, the stronger is the deceleration. At Houtrib station the wind speed is very close to that over the sea. That is explained by the fact that the air flow decelerates over the land and accelerates running over the lake. The fetch appears to be long enough for the wind speed to reach the values observed over the sea.

In Figures 6 and 7 'sea wind speed' against observed 'land wind speed' (left columns) is plotted for each of the stations. The plots clearly reveal the features of the wind transformation mentioned above. In Table l the regression coefficient A, the standard deviation, and the standard error of A, ΔA are presented

$$U_{sea} = AU_{land}, \tag{55}$$

where

$$A = \frac{\sum U_{sea_i} U_{land_i}}{\sum U^2_{land_i}}, \tag{56}$$

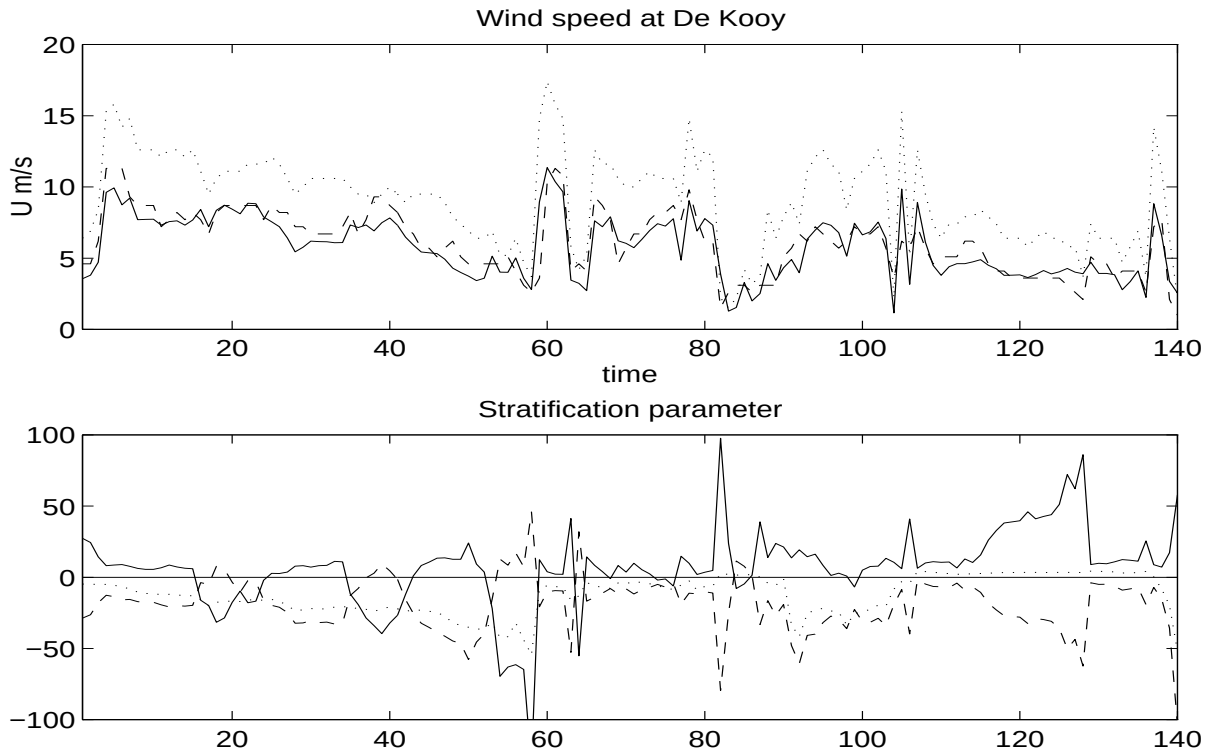

Figure 2: Upper panel. Series of subsequent cases of the wind speed at De Kooy station, when the wind direction happens to be in the right interval. Solid line, modelled; dashed line, observed over the land; dotted line, observed over the sea. Lower panel. Series of the stratification parameter μ. Solid line, over the land; dotted line, over the sea; dashed line, of the sea- land transition according to (54).

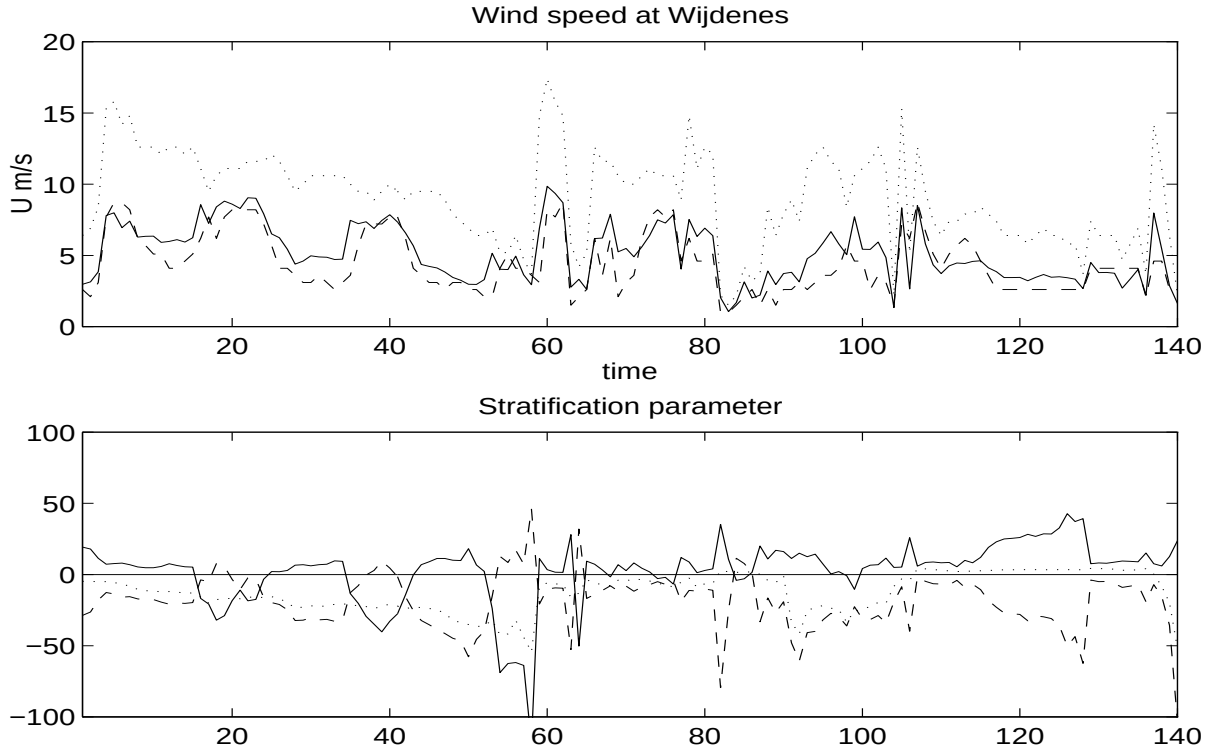

Figure 3: Upper panel. The same as in Figure 2 but for Wijdenes station. Solid line, modelled; dashed line, observed over the land; dotted line, observed over the sea. Lower panel. Series of the stratification parameter μ. Solid line, over the land; dotted line, over the sea; dashed line, of the sea-land transition according to (54).

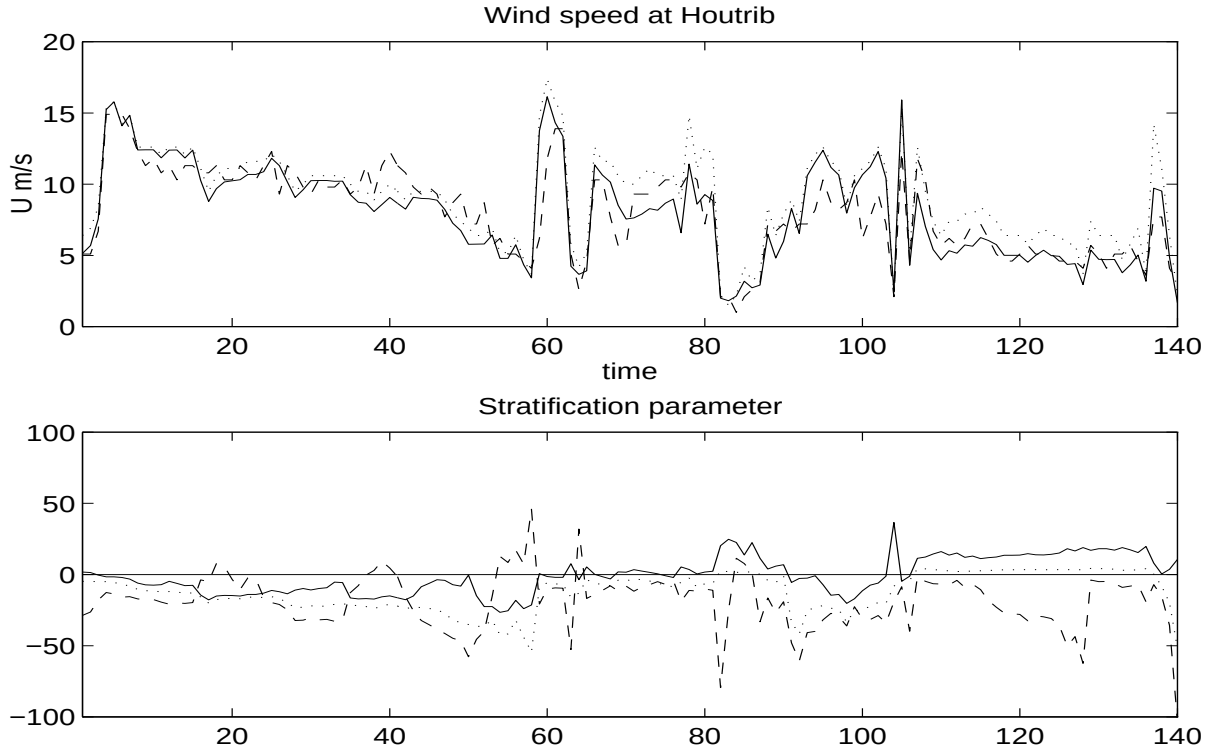

Figure 4: Upper panel. The same as in Figure 2 but for Houtrib station. Solid line, modelled; dashed line, observed over the land; dotted line, observed over the sea. Lower panel. Series of the stratification parameter μ. Solid line, over the land; dotted line, over the sea; dashed line, of the sea- land transition according to (54).

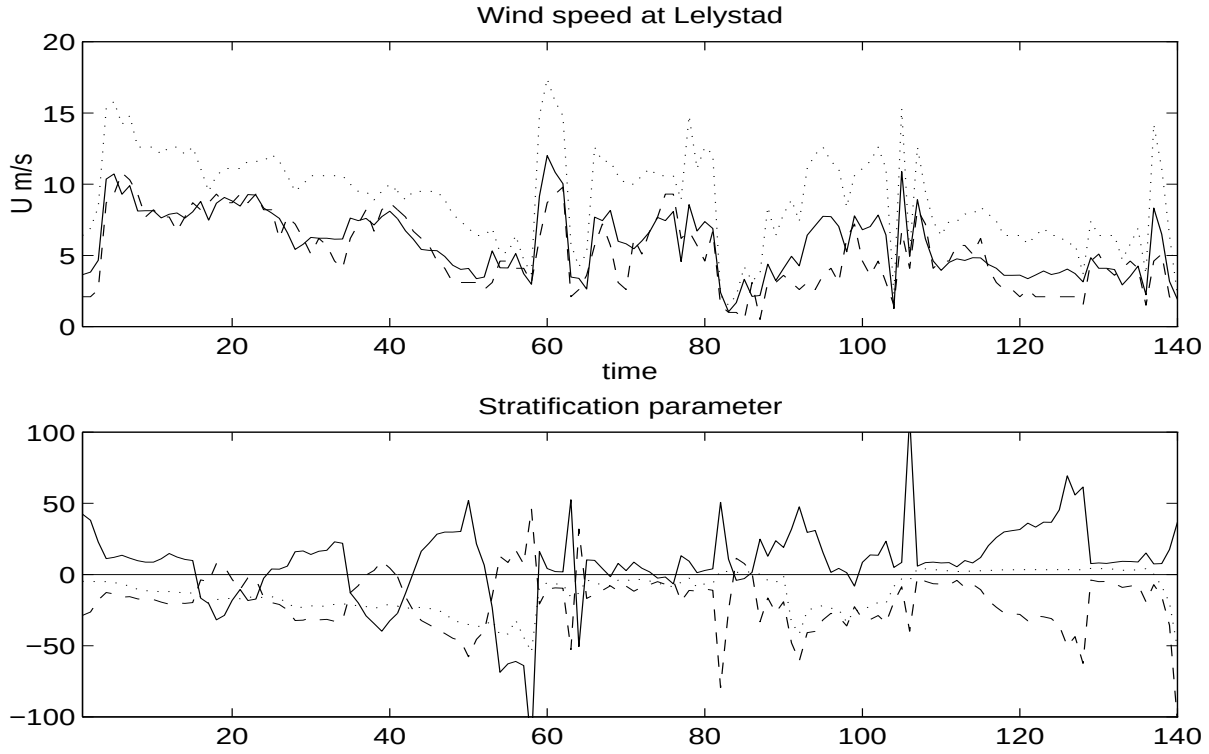

Figure 5: Upper panel. The same as in Figure 2 but for Lelystad station. Solid line, modelled; dashed line, observed over the land; dotted line, observed over the sea. Lower panel. Series of the stratification parameter μ. Solid line, over the land; dotted line, over the sea; dashed line, of the sea-land transition according to (54).

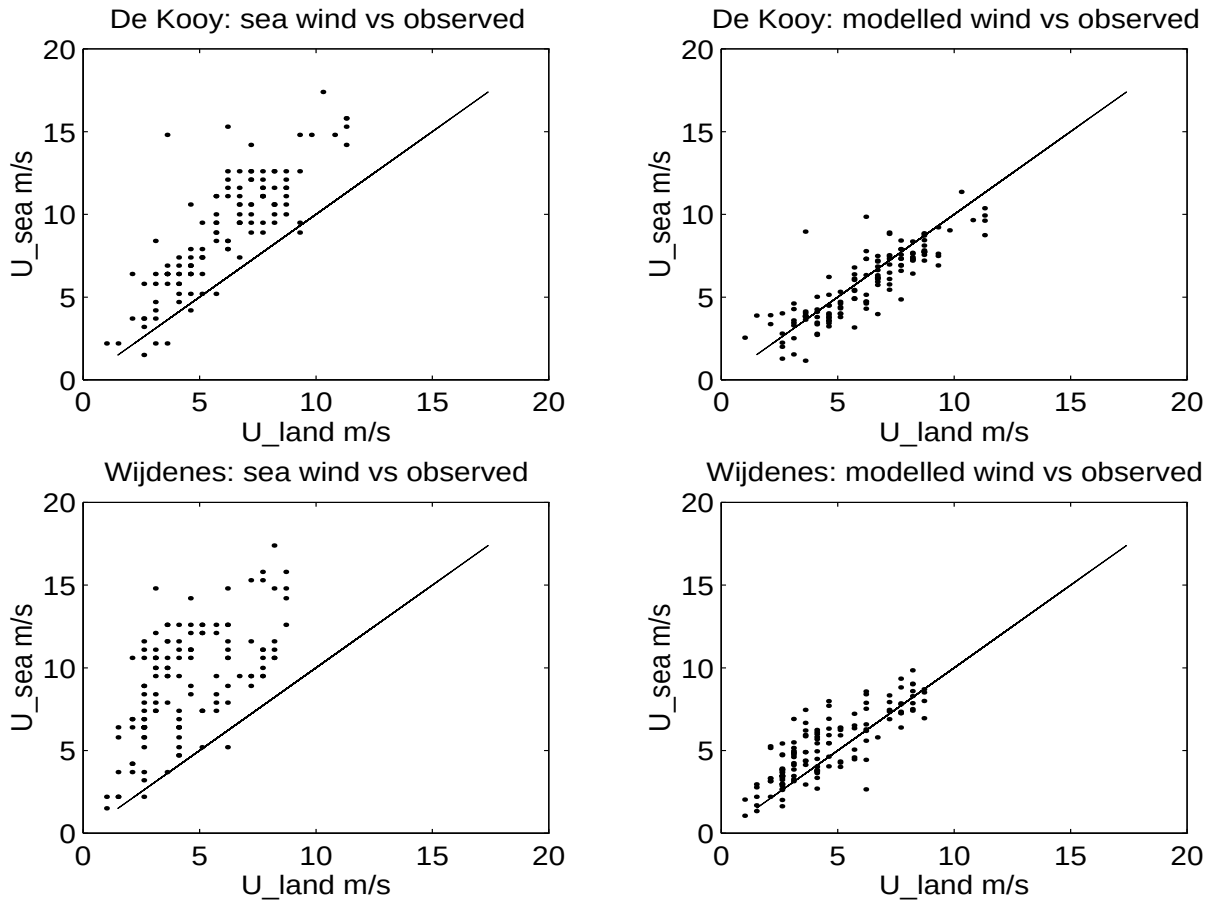

Figure 6: Upper panel. Wind speed at De Kooy station. Left, sea wind speed versus observed wind speed over land; right, modelled wind speed versus observed wind speed over land. Lower panel. The same, but at Wijdenes station.

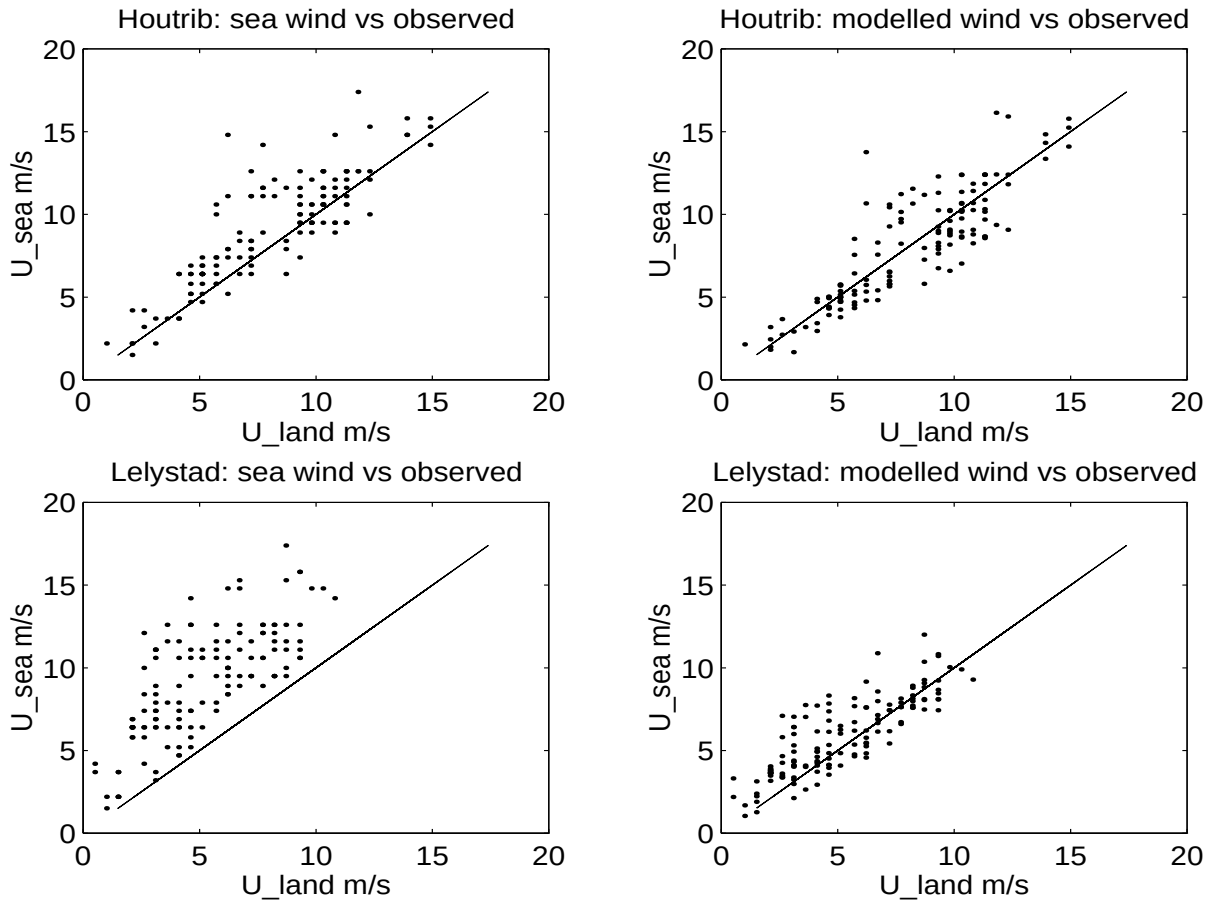

Figure 7: Upper panel. Wind speed at Houtrib station. Left, sea wind speed versus observed wind speed over land; right, modelled wind speed versus observed wind speed over land. Lower panel. The same, but at Lelystad station.

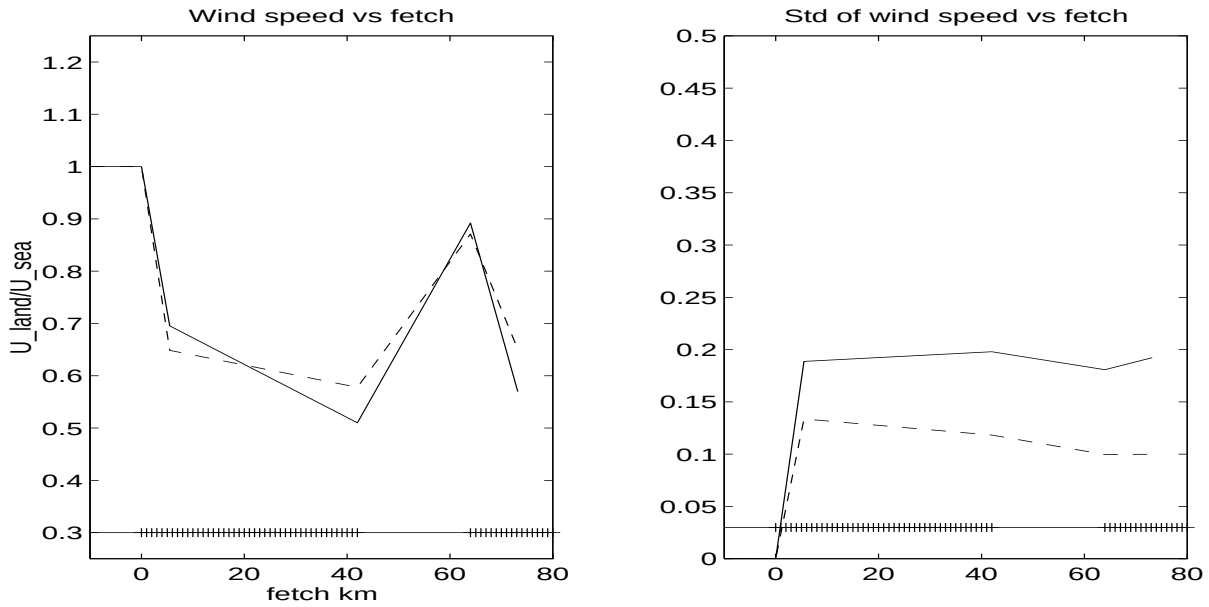

Figure 8: Left. Wind speed normalized by the wind speed over the sea as a function of fetch along De Kooy - Wijdenes - Houtrib - Lelystad. Solid line, observed; dashed line, modelled. The shaded intervals correspond to the transition De Kooy-Wijdenes, and Houtrib-Lelystad. Right. The same, but for the standard deviation.

and

$$\Delta A = \frac{\sum (U_{sea_i} - A U_{land_i})^2}{\sum U_{land_i}^2}. \tag{57}$$

The deceleration of the air flow over the rough land results in $A > 1$; the longer the fetch, the

Station	De Kooy	Wijdenes	Houtrib	Lelystad
A	1.46	1.86	1.11	1.60
Std in m/s	1.5	3.1	1.8	2.8
ΔA	0.02	0.06	0.02	0.04
$\Delta A/A(\%)$	1.6	3.0	1.6	2.6

Table 1: Regression coefficient A, standard error of A - ΔA, and the standard deviation between observed wind speed over sea and land.

higher is the value of A. According to observations the wind speed at Wijdenes is half that of the wind speed over the sea. The wind speed measured at Houtrib station is approximately equal to the sea wind speed.

3.3 Model Results and Comparison With Measurements

The model described in Section 2 is used here to reproduce the observations. The model is used in the multi-transitional regime. The spatial scales i.e., the fetch over the land, the lake and again over the land were determined for the selected wind direction. The external parameters used for calculations (see Section 3.1) are: the coastal wind speed at 18 m height, the air temperature at 850 mbar, the sea surface temperature, the lake surface temperature, and the land roughness parameter.

To run the model the land surface temperature must be specified. The soil temperature at some depth (5 or 10 cm) is not appropriate for this purpose, because the turbulent regime of the stratified boundary layer is affected by the surface temperature which can differ significantly from the soil temperature. For example, due to the absorption of the solar radiation the surface land temperature could be significantly higher than the soil temperature. We thus reconstruct the land temperature from the observed at two levels air temperature by the procedure described in Appendix 6.3.

The modelled and observed wind speed for the subsequent cases when the wind direction happens to be in the right interval are shown in Figures 2-5. In general the agreement between modelled and observed wind speed is rather encouraging. The model prediction of the sharp decrease in the wind speed due to deceleration of the air flow over the rough land is quantitatively consistent with the observed trends. The model predicts acceleration of the air flow over the lake as well. The most important observed and predicted feature is the explicit correlation of the wind speed with the stratification parameter of the atmospheric boundary layer. For example, the series at Wijdenes (Figure 3) show quasi-periodical variations of the wind speed in the period marked by 5 to 55. These variations are not caused by variations in the background sea wind speed (which rather show an opposite behaviour), but are well correlated with the stratification parameter. This effect may be interpreted as follows. When stratification is unstable, strong vertical turbulent mixing causes an increase of the wind speed. The suppression of turbulent mixing in a stably stratified boundary layer results in a decrease of the wind speed. These important features are well reproduced by the model.

In Figures 6 and 7 (right columns) the modelled wind speed is plotted against observed wind speed. As a rule the dots are scattered along the bisector line, showing a good model performance. In Table 2 the regression coefficient, the standard error, and the standard deviation are presented. Regression coefficients are close to 1. That shows that the model is able to reproduce the observed decrease of the wind speed over the land and its increase over the Markermeer lake quantitatively well. The standard deviation and the standard error ΔA between modelled and observed wind speed is even less than that between the observed sea and land winds. However, the relative error $\Delta A/A$ does not decrease considerably. We could anticipate that including stratification effects into the model would improve the correlation between the measured and observed wind speed at inland stations. That would be true if the scatter in the data was caused by stratification effects. However, this seems not to be the case here. If the scatter in Figures 6 and 7, left columns, would be caused by stratification, it should be reduced with increasing wind speed. Such a tendency is not seen in the figures. The scatter is most probably caused by the synoptic variability of the atmosphere.

Station	De Kooy	Wijdenes	Houtrib	Lelystad
A	0.93	1.10	0.99	1.07
Std in m/s	1.1	1.4	1.5	1.7
ΔA	0.01	0.02	0.02	0.02
$\Delta A/A(\%)$	1.6	2.1	1.7	2.1

Table 2: Regression coefficient A, standard error of A - ΔA, and the standard deviation between modelled and observed wind speed.

In Figure 8, observed and modeled wind speeds normalized by the sea wind speed are shown as a function of the fetch. Each point is obtained by the time average of observed or modelled wind speeds at stations. For clarity's sake the points are connected by lines. Notice, that between the land stations the roughness parameter is kept constant, so that lines represent the wind transformation along the homogeneous surfaces. The figure clearly shows how the air flow formed over the North Sea is transformed over North Holland. Reaching the land at De Kooy the wind decelerates sharply. It is very interesting to see that within a few kilometres (coastline - De Kooy), according to the observations and the model, the boundary layer has been adapted to typical land conditions; useful to realise for people who may think that De Kooy is representative for the nearby sea area. After 40 km at Wijdenes the wind speed has been reduced to half its value over the sea. The wind sharply accelerates over the Markermeer lake, almost recovering to the level of the wind speed over the sea. This sharp acceleration is explained by the fact that the sea roughness is much smaller than the land roughness and, moreover, the unstable conditions above the lake are favourable for the fast growth of the boundary layer. The wind velocity drops again running into Flevoland. The model predictions are fully consistent with measurements. This fact is encouraging and shows that the simplified model can be useful in applied studies of the wind transformation.

4 Conclusions

A simplified model of the PBL transformation caused by abrupt changes in surface roughness and temperature is presented. The model is based on the concept of Internal Boundary Layer growth. The proposed equation for the growth rate of the IBL height is valid for both small scale and mesoscale IBL evolution and can be used for IBLs of arbitrary stratification. A similarity approach is used to describe the structure of the IBL developing inside the surface boundary layer. The description of the Ekman part of the IBL is based on the assumption that the turbulent transfer coefficient is independent of height and equals to its value at the upper boundary of the SBL. The fetch dependence of the IBL structure is taken into account implicitly via the fetch dependence of heat and momentum fluxes which, in turn, are defined by the resistance laws.

The model describes the transformation of wind across a coastal line (off-shore and on-shore winds) and across land-sea-land or sea-land-sea domains. The model has been verified

against wind speed observations collected at four stations in North Holland in the period August 1994 - January 1995. Overall, a good agreement between modelled and observed wind speed is obtained. It is concluded that the model is capable to predict the main features of the wind transformation above complex terrains characterized by variable roughness and surface temperature and thus is a useful tool for applied and engineering studies.

5 Acknowledgments

The first author is grateful for the financial support he received from the Royal Netherlands Meteorological Institute (KNMI). The support from EU INTAS-International Association under the project INTAS-96-1817 is acknowledged by VNK and VKM. The authors would like to thank Jeanette Onvlee, Evert Bouws, and Wim de Rooy for useful comments.

6 Appendix

6.1 Universal Dimensionless Functions

The dimensionless profile functions of Monin-Obukhov similarity theory Ψ_i, $i = [u, \theta]$ are related to the dimensionless gradients Φ_i by

$$\Phi_i(z/L) = 1 - \Psi_i'(z/L)\frac{z}{L}. \tag{58}$$

The dimensional gradients are defined by

$$\frac{\partial U}{\partial z} = \frac{u_*}{\kappa z}\Phi_u(z/L), \tag{59}$$

$$\frac{\partial \Theta}{\partial z} = \frac{\theta_*}{\kappa z}\Phi_\theta(z/L) \tag{60}$$

and are related to the eddy-viscosity K_i by

$$K_i = \frac{u_*\kappa z}{\Phi_i(z/L)}. \tag{61}$$

The dimensionless gradients are determined empirically from the flux-profile relations (59), (60). Widely accepted functional relations are (Dyer, 1974; Yaglom, 1977):

$$\Phi_u(z/L) = \left(1 - C_1\frac{z}{L}\right)^{-1/4}, \quad z/L < 0, \tag{62}$$

$$\Phi_u(z/L) = 1 + C_2\frac{z}{L}, \quad z/L > 0. \tag{63}$$

We use $C_1 = 16$ and $C_2 = 5$. For temperature the gradient relations are

$$\Phi_\theta(z/L) = \left(1 - C_3\frac{z}{L}\right)^{-1/2}, \quad z/L < 0, \tag{64}$$

$$\Phi_\theta(z/L) = 1 + C_4\frac{z}{L}, \quad z/L > 0, \tag{65}$$

and it is normally assumed that $C_3 = C_1$ and $C_4 = C_2$.

The profile dimensionless functions are then

$$\Psi_u(z/L) = 2\ln\frac{1+X}{2} + \ln\frac{1+X^2}{2} - 2\tan^{-1}X + \frac{\pi}{2}, \quad z/L < 0, \tag{66}$$

$$\Psi_u(z/L) = -C_2\zeta, \quad z/L > 0, \tag{67}$$

$$\Psi_\theta(z/L) = 2\ln\frac{1+X^2}{2}, \quad z/L < 0, \tag{68}$$

$$\Psi_\theta(z/L) = -C_4\frac{z}{L}, \quad z/L > 0, \tag{69}$$

where $X = (1 - C_1 z/L)^{1/4}$.

6.2 Parameters of Background PBL Reconstructed From Measurements

Measurements of wind velocity and air temperature are usually performed at different levels above the surface. Here, the procedure to obtain the PBL parameters based on such measurements is described. Let Z_u and Z_θ be the levels where wind velocity and air temperature are measured. Their measured values are $\mathbf{U}_Z$ and θ_Z respectively, and they are related to wind and temperature profiles (6) and (7), or (8) and (9) depending on the relation between Z_u, Z_θ and h. We first define the surface heat and momentum fluxes from measured wind speed and temperature. They follow from modified resistance laws

$$\frac{\kappa\mathbf{U}_Z}{\mathbf{u}_*} = \ln\left(\frac{Z_u}{z_0}\right) - \Psi_u\left(\frac{Z_u}{L}\right), \tag{70}$$

$$\frac{\kappa(\theta_Z - \theta_s)}{\theta_*} = \ln\left(\frac{Z_a}{z_{0t}}\right) - \Psi_\theta\left(\frac{Z_u}{L}\right) \tag{71}$$

if Z_u and/or Z_a are less than h. If Z_u and/or Z_a exceed h then the resistance laws are

$$\frac{\kappa(\theta_Z - \theta_s)}{\theta_*} = \ln\left(\frac{\kappa u_*}{f z_{0t}}\right) - C(\mu, Z_a), \tag{72}$$

$$\frac{\kappa\mathbf{U}_Z}{\mathbf{u}_*} = \ln\left(\frac{\kappa u_*}{f z_0}\right) - B(\mu, Z_u) - iA(\mu, Z_u), \tag{73}$$

where $A(\mu, Z_u)$, $B(\mu, Z_u)$, and $C(\mu, Za)$ are universal functions defined as

$$A(\mu, Z_u) = \Lambda^{-1}(\mu)\frac{\sinh((1+i)(m-\varepsilon)) - \sinh((1+i)(m - Z_u/H))}{\cosh((1+i)(m-\varepsilon))}, \tag{74}$$

$$B(\mu, Z_u) = -A(\mu, Z_u) + \Psi_u(\varepsilon\mu\Lambda(\mu)) - \ln(\varepsilon\Lambda(\mu)), \tag{75}$$

$$C(\mu, Z_a) = -2\Lambda^{-1}(\mu)(Z_a/H - \varepsilon) + \Psi_\theta(\varepsilon\mu\Lambda(\mu)) - \ln(\varepsilon\Lambda(\mu)). \tag{76}$$

These equations can be solved iteratively to obtain the surface heat and momentum fluxes via the measured wind speed and air temperature. As soon as they are found the wind velocity and temperature profiles in the background PBL obviously follow from (6) and (7) or, (8) and (9).

6.3 Determination of Land Temperature From Measurements of Air Temperature at Two Levels

Knowledge of the land temperature plays a crucial role in the description of the IBL evolution. However, measurements of the surface temperature are usually not available. The soil temperature (at $z = -5$ cm) gives only an estimate of the real surface temperature, which can be significantly affected by solar irradiation. At the same time measurements of air temperature are usually available at two levels. We consider here the case when the observed temperature is available from two levels $Z_1 = 1.5$m and $Z_2 = 850$ mbar. Under all conditions the former level is located in the SBL while the latter is well inside the Ekman part of the PBL. The vertical distribution of temperature inside the SBL is

$$\theta(z) = \theta_s + \frac{\theta_*}{\kappa}\left[\ln(\frac{z}{z_0 t}) - \Psi_\theta(z/L)\right],$$

and inside the Ekman part of the PBL is

$$\theta(z) - \theta_2 = -2\frac{\theta_*}{\kappa}\Lambda^{-1}\frac{Z_2 - z}{H}.$$

The temperature difference at level z and Z_1 confined to the SBL is

$$\theta(z) - \theta_1 = \frac{\theta_*}{\kappa}\left[\ln(\frac{z}{Z_1}) - \Psi_\theta(z/L) + \Psi_\theta(Z_1/L\right].$$

The last two equations being patched at $z = h$ (we remind that $Z_1 < h < Z_2$) give the resistance law

$$\frac{\kappa(\theta_2 - \theta_1)}{\theta_*} = \ln\left(\frac{h}{Z_1}\right) - \Psi_\theta\left(\frac{h}{L}\right) + \Psi_\theta\left(\frac{Z_1}{L}\right) + 2\Lambda^{-1}(\mu)\frac{Z_2 - h}{H}$$

which has to be considered along with the resistance law for the friction velocity (70). After the surface heat and momentum fluxes are found the unknown land temperature follows from

$$\theta_s = \theta_1 - \frac{\theta_*}{\kappa}\left[\ln(\frac{Z_1}{z_0 t}) - \Psi_\theta(Z_1/L)\right].$$

References

[1] Belcher, S.E. and J.C.R. Hunt: 1993, 'Turbulent shear flow over slowly moving waves', J. Fluid Mech., **251**, 109-148.

[2] Bergstrom, H.A.: 1985, 'Simplified boundary layer wind model for practical applications', *J. Clim. Appl. Meteorol.*, **25**, 813-823.

[3] Bergstrom, H.A., Johansson, P.E., and A.S. Smedman: 1988, 'A study of wind speed modification and internal boundary layer heights in a coastal region', *Boundary-Layer Meteorol.*, **42**, 313-335.

[4] Brown, R. A.: 1982, 'On two-layer models and the similarity functions for the PBL', *Boundary- Layer Meteorol.*, **24**, 451-463.

[5] Bradley E.F.: 1968, 'A micrometeorological study of velocity profiles and surface drag in the region modified by a change in surface roughness', *Quart. J. Roy. Meteorol. Soc.*, **94**, 361-379.

[6] Charnock, H.: 1955, 'Wind stress on a water surface', *Quart. J. Roy. Meteorol. Soc.*, **81**, 639-640.

[7] Deardorff, J.W.: 1972, 'Numerical investigation of neutral and unstable planetary boundary layers', *J. Atmos. Sci.*, **29**, 91-115.

[8] Dyer, A.J.: 1974, 'A review of flux-profile relations', *Boundary-Layer Meteorol.*, **7**, 363-372.

[9] Elliot, W.P.: 1958, 'The growth of the atmospheric internal boundary layer', *Trans. Amer. Geophys. Un.*, **39**, 1048-1054.

[10] Garratt J.R.: 1987, 'The stable stratified internal boundary layer for steady and diurnally varying offshore flow', *Boundary- Layer Meteorol.*, **38**, 369-394.

[11] Garratt, J.R.: 1990, 'The Internal Boundary Layer - A review', *Boundary-Layer Meteorol.*, **50**, 171-203.

[12] Garratt, J.R. and B.F.Ryan: 1989, 'The structure of the stably stratified internal boundary layer in offshore flow over the sea', *Boundary-Layer Meteorol.*, **47**, 17-40.

[13] Garratt, J.R., Hess, G.D., Physick, W.L. and P. Bougeault: 1996, 'The atmospheric boundary layer - advances in knowledge and application', *Boundary-Layer Meteorol.*, **78**, 9-37.

[14] Jensen S.E., Petersen E.L. and I. Troen: 1984, 'Extrapolation of mean wind statistics with special regard to wind energy applications', *World Meteorol.Org.*, **WCP-86**, 85 pp.

[15] Kazansky, A.B. and Monin, A.S.: 1960, 'On turbulent regime above near-surface air layer', *Izv. Akad. Nauk SSSR, Ser. Geophys.*, **1**, 165-168.

[16] Kudryavtsev, V.N.: 1995, 'A model of atmosphere boundary layer transformation above sea surface temperature front', *Morskoy Hydrof. Zurnal*, **2**, 24-51.

[17] Kudryavtsev, V and V. Makin: 1996, 'Transformation of wind in the coastal zone', KNMI, Scientific Report, WR 96-04, 57pp.

[18] Kudryavtsev, V., S. Grodsky, V. Dulov, and V. Malinovsky: 1996, 'Observation of atmospheric boundary layer evolution above the Gulf Stream frontal zone', Boundary Layer Met., 79, 51-82.

[19] Mason, P.J.: 1994, 'Large-eddy simulation: a critical review of the technique', *Quart. J. R. Meteorol. Sci.*, **120**, 1-26.

[20] Meroney, R.W., Cermak, J. E. and Yang, B.T.: 1975, 'Modeling of atmospheric transport and fumigation at shoreline sites', *Boundary-Layer Meteorol.*, **9**, p.69-90.

[21] Monin, A.S. and Obukhov, A.M.: 1954, 'Main laws of turbulent mixing in near-surface layer of atmosphere', *Trudy Geophys. Inst. Akad. Nauk*, **24(151)**, 163-187.

[22] Mulhearn P.J.: 1977, 'Relations between surface fluxes and mean profiles of velocity, temperature and concentration, downwind of a change in surface roughness' *Quart. J. Roy. Meteorol. Soc.*, **103**, 785-802.

[23] Mulhearn, P.J.: 1981, 'On the formation of a stably stratified internal boundary layer by advection of warm air over a cooler sea', *Boundary-Layer Meteorol.*, **21**, 247-254.

[24] Panofsky, H. and J. Dutton: 1984, *Atmospheric Turbulence*, Academic, San Diego, Calif., 397 pp.

[25] Raynor G.S., P. Michael, R.M.Brown, and S. Sethuraman: 1975, 'Studies of atmospheric diffusion from a nearshore oceanic site', *J. Appl. Meteorol.*, **7**, 331-348.

[26] Raynor, G.S., Sethuraman, S. and Brown, R.M.: 1979, 'Formation and characteristics of coastal internal boundary layers during onshore flows' *Boundary-Layer Meteorol.*, **16**, 487-514.

[27] Rossby C.G. and Montgomery R.: 1935, 'The layers of frictional influence in wind ocean currents', *MIT paper* **3**, 3-101.

[28] Schlichting, H.: 1979, *Boundary Layer Theory*, McGrow-Hill, New York and London, 817 pp.

[29] Tennekes H.: 1973, 'A model for the dynamics of the inversion above a convective boundary layer', *J. Atmos. Sci.*, **30**, 558-567.

[30] Townsend A.A.: 1965, 'The response of a turbulent boundary layer to abrupt changes in surface conditions', *J. Fluid Mech.*, **22**, 799-822.

[31] Taylor P.A.: 1971, 'Airflow above changes in surface heat flux, temperature and roughness: An extension to include the stable case', *Boundary-Layer Meteor.*, **1**, 474-497.

[32] Taylor P.A. and R.J. Lee: 1984, 'Simple guidelines for estimating wind speed variations due to small scale topographic feature', *Climatol. Bull. Canadian Meteorol. Oceanogr. Soc.*, **18**, 3-32.

[33] Van Wijk A.J.M., A.C.M. Beljaars, A.A.M. Holtslag and W.C. Turkenburg: 1990, 'Diabatic wind speed profiles in coastal regions: comparison of an internal boundary layer (IBL) model with observations', *Boundary-Layer Meteorol.*, **51**, 49-75.

[34] Venkatram A.A.: 1977, 'Model of internal boundary-layer development', *Boundary-Layer Meteorol.*, **11**, 419-438.

[35] Walmsley J.L.: 1989, 'Internal boundary layer height formulate - A comparison with atmospheric data', *Boundary- Layer Meteorol.*, **47**, 251-262.

[36] Zilitinkevich, S.S.: 1970, *Dynamics of the Atmospheric Boundary Layer*, Gidrometeoizdat, Leningrad, 292 pp.

[37] Zilitinkevich, S.S.: 1989a, 'Velocity profiles, resistance law and the dissipation rate of mean flow kinetic energy in a neutrally and stably stratified Planetary Boundary Layer', *Boundary-Layer Meteorol.*, **46**, p.367-387.

[38] Zilitinkevich, S.S.: 1989b, 'The temperature profile and heat transfer law in neutrally and stably stratified Planetary Boundary Layer', *Boundary-Layer Meteor.*, **49**, 1-6.

[39] Yaglom, A.M.: 1977, 'Comments on wind and temperature flux-profile relationships', *Boundary-Layer Meteor.*, **11**, 89-102.